Chemosphere 320 (2023) 138093

Contents lists available at ScienceDirect

Chemosphere

journal homepage: www.elsevier.com/locate/chemosphere

Identifying antimicrobials and their metabolites in wastewater and surface water with effect-directed analysis

Tim J.H. Jonkers [a], Peter H.J. Keizers [b], Frederic Béen [a,c], Jeroen Meijer [a,d], Corine J. Houtman [e], Imane Al Gharib [f], Douwe Molenaar [f], Timo Hamers [a], Marja H. Lamoree [a,*]

[a] Department of Environment & Health, Faculty of Science, Amsterdam Institute for Life and Environment, Vrije Universiteit Amsterdam, De Boelelaan 1085, 1081 HV, Amsterdam, the Netherlands
[b] National Institute for Public Health and the Environment RIVM, A. van Leeuwenhoeklaan 9, 3721MA, Bilthoven, the Netherlands
[c] KWR Water Research Institute, Groningenhaven 7, 3430 BB, Nieuwegein, the Netherlands
[d] Institute for Risk Assessment Sciences (IRAS), Utrecht University, Yalelaan 2, 3584 CM, Utrecht, the Netherlands
[e] The Water Laboratory, J.W. Lucasweg 2, 2031 BE, Haarlem, the Netherlands
[f] Systems Biology Lab, Faculty of Science, Amsterdam Institute for Life and Environment, Vrije Universiteit Amsterdam, De Boelelaan 1085, 1081 HV, Amsterdam, the Netherlands

HIGHLIGHTS

- An antibiotic bioassay confirmed bioactive fractions in fractionated water samples.
- Chemical features related to bioactivity were prioritized for identification.
- Phase I metabolites were predicted *in silico* for over 500 antibiotics.
- A bioactive metabolite was identified as 14-OH(R) clarithromycin.
- 78% of the measured bioactivity was explained by the identified compounds.

GRAPHICAL ABSTRACT

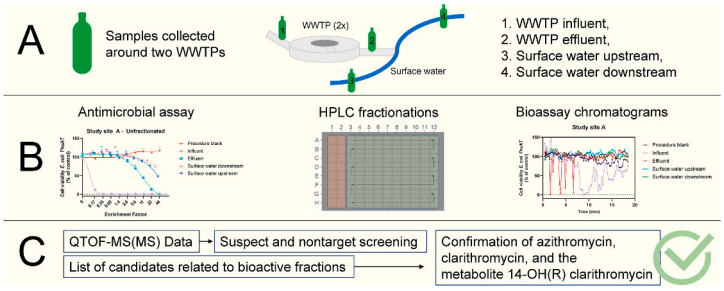

ARTICLE INFO

Handling Editor: Keith Maruya

Keywords:
Antibiotic
Effect-directed analysis
Clarithromycin
Bioassay
Metabolite
Nontarget screening

ABSTRACT

This study aimed to identify antimicrobial contaminants in the aquatic environment with effect-directed analysis. Wastewater influent, effluent, and surface water (up- and downstream of the discharge location) were sampled at two study sites. The samples were enriched, subjected to high-resolution fractionation, and the resulting 80 fractions were tested in an antibiotics bioassay. The resulting bioactive fractions guided the suspect and non-targeted identification strategy in the high-resolution mass spectrometry data that was recorded in parallel. Chemical features were annotated with reference databases, assessed on annotation quality, and assigned identification confidence levels. To identify antibiotic metabolites, Phase I metabolites were predicted *in silico* for over 500 antibiotics and included as a suspect list. Predicted retention times and fragmentation patterns reduced the number of annotations to consider for confirmation testing. Overall, the bioactivity of three fractions could be explained by the identified antibiotics (clarithromycin and azithromycin) and an antibiotic metabolite (14-OH(R) clarithromycin), explaining 78% of the bioactivity measured at one study site. The applied identification strategy

* Corresponding author.
E-mail addresses: tim.jonkers@vu.nl (T.J.H. Jonkers), peter.keizers@rivm.nl (P.H.J. Keizers), frederic.been@kwrwater.nl (F. Béen), j.meijer@vu.nl (J. Meijer), corine.houtman@hetwaterlaboratorium.nl (C.J. Houtman), d.molenaar@vu.nl (D. Molenaar), timo.hamers@vu.nl (T. Hamers), marja.lamoree@vu.nl (M.H. Lamoree).

https://doi.org/10.1016/j.chemosphere.2023.138093
Received 12 December 2022; Received in revised form 4 February 2023; Accepted 6 February 2023
Available online 7 February 2023

successfully identified antibiotic metabolites in the aquatic environment, emphasizing the need to include the toxic effects of bioactive metabolites in environmental risk assessments.

1. Introduction

Due to their inadequate removal in wastewater treatment plants (WWTPs), antibiotics are introduced into the aquatic environment mainly by WWTP effluent discharges (Wang et al., 2020). The presence of antimicrobial contaminants has led to environmental health concerns regarding their adverse health effects on nontarget organisms in the environment (EC, 2019; Fu et al., 2017) and human health concerns regarding the development and transfer of antibiotic resistance (Bengtsson-Palme and Larsson, 2016; Wengenroth et al., 2021). To protect the quality of surface water bodies that are often also used for drinking water production, there is a need to identify toxic environmental contaminants and determine their associated risks (Escher et al., 2020; Loos et al., 2018).

Biological and chemical screening techniques are often used in parallel to assess water quality (Hamers et al., 2015; Neale et al., 2017; Serra-Compte et al., 2021). Their parallel use has shown that often only a small fraction of the observed toxicity in a bioassay can be explained by the chemicals identified with targeted screening techniques (Escher et al., 2020; Hamers et al., 2015; Houtman et al., 2018; Neale et al., 2017). Part of this unexplained activity may be attributed to bioactive transformation products (including metabolites) (Escher and Fenner, 2011; Hamers et al., 2015; Petrie et al., 2015), which are often not included in the targeted chemical analysis. Also, compounds with previously unknown activity can contribute to toxicity (Zwart et al., 2018).

This study aimed to identify active antimicrobial compounds, including antibiotics and their metabolites, in extracts from WWTP influent, WWTP effluent, and receiving surface water (up and downstream of the discharge locations). To the authors' knowledge, EDA has not yet been applied to identify antimicrobial compounds in these sample types. Samples were collected at two study sites and analyzed according to a recently developed workflow for the high-throughput identification of bioactive contaminants with effect-directed analysis (EDA) (Jonkers et al., 2022). The complex mixtures of contaminants present in the water extracts were separated by reversed-phase liquid chromatography (LC) and collected into fractions, resulting in less complex chemical mixtures (i.e. fewer compounds). Fractions were tested for their antimicrobial activity in an antibiotics bioassay (Jonkers et al., 2020). In addition, high-resolution mass spectrometry (HRMS) was used to detect chemical features (accurate chemical masses) in the extracts. Finally, the features with retention times similar as the bioactive fractions were annotated with mass spectral libraries, suspect screening lists, and targeted screening libraries of analytical standards. To specifically target antibiotic metabolites, human Phase I antibiotic metabolites were predicted *in silico* and included as a suspect screening list.

2. Materials and methods

2.1. Sample locations and extraction

Water samples were collected at two WWTPs in the Netherlands, located in Utrecht (study site A, 52°06′42.9″N 5°06′27.9″E) and Nieuwegein (study site B, 52°00′13.8″N 5°04′16.6″E). Both WWTPs receive communal wastewater including hospital wastewater, which may possibly increase the antimicrobial potency of the samples and lead to an increased identification rate of bioactive compounds. Two WWTPs were selected to gain a clearer understanding of the presence of bioactive contaminants in the water samples under study, in part by comparing the presence of identified contaminants between the two plants. The capacity of the WWTPs is 430,000 person equivalents (PE) for study site A and 144,000 PE for study site B. Four samples were collected for each study site: a 24-h composite influent sample, a 24-h composite effluent sample, a surface water grab sample ~2 km upstream, and a surface water grab sample ~1 km downstream of the effluent discharge location. The samples were collected in May 2019 for study site A and in September 2019 for study site B. Samples were kept frozen (−20 °C) until further processing. After thawing the samples, EDTA was added to 500 mL of each sample as a chelating agent at a final concentration of 100 μM, to improve the extraction recoveries of antibiotics (Gros et al., 2013). The samples were filtered through a 0.7 μM glass fiber filter (Whatman GF/F) and acidified to pH 3.0 with formic acid (BioSolve, Valkenswaard, The Netherlands). Solid-phase extraction was performed with OASIS HLB cartridges (500 mg, 6 cc). After elution with methanol (BioSolve, Valkenswaard, The Netherlands) (3 × 3 mL), the extract was split into 2 parts in a 1:5 ratio, meant for bioassay testing of unfractionated extracts and for chemical analysis and fractionation, respectively. The extracts were concentrated using evaporation of solvents in a water bath at 40 °C and reconstituted in 50 μL DMSO for bioassay testing (Acros, Geel, Belgium) or 250 μL in 50% (v/v) methanol in Milli-Q for chemical analysis and fractionation (water purified on a Milli-Q Reference A+ purification system (Millipore, Bedford, MA)). The suitability of the sample preparation, separation, and detection method was determined for 13 antibiotics in a separate verification experiment that is described in Section S4 of the Supporting Information.

2.2. Chemical analysis and fractionation

LC and HRMS analyses and high-resolution fractionation were performed as described in Jonkers et al. (2022). In short, 20 μL of sample extract (in 50% (v/v) methanol in Milli-Q) was injected with an Agilent 1290 Infinity HPLC system (Agilent Technologies, Amstelveen, The Netherlands) onto a BEH C18 column (Waters, 100 mm × 2.1 mm, 2.5 μm) set to 30 °C. Milli-Q with 0.1% formic acid (v/v) and acetonitrile (ACN) with 0.1% formic acid (v/v) were used as mobile phases. Compounds were separated at a flow rate of 0.5 mL/min with a linear gradient. The gradient was increased from 10% ACN (0.1% formic acid (v/v)) to 99% ACN (0.1% formic acid (v/v)) in 18 min, kept there for 7.5 min, and returned to 10% ACN (0.1% formic acid (v/v)) in the next 0.5 min. The subsequent equilibration time of the column was 4 min. HRMS data were acquired on a Bruker Compact II QTOF mass spectrometer (Bruker, Bremen, Germany) equipped with an electrospray ionization source operated in positive and negative ion mode. Full scan (MS) and MS/MS scans were recorded for masses from 50 to 1300 m/z at scan rates of 2 Hz and 5 Hz, respectively, with single injections. MS/MS data were acquired in data-dependent acquisition mode. Before fractionation, 10 μL of 10% DMSO (in Milli-Q) was added to each well of a clear polystyrene F-bottom 96-well plate (Greiner Bio-One) as keeper solvent. Samples were fractionated with a FractioMate™ (SPARKHolland & VU, Emmen & Amsterdam, the Netherlands) (Jonker et al., 2019) that collected 80 fractions of 13.5-s intervals in wells A3-H12 of the plate under the same HPLC conditions as the chemical analysis (Fig. S1), corresponding to the linear gradient of the elution program. The fractionation procedure is described in detail in the Supporting Information (Section S1). Post-fractionation, the solvents were evaporated in a CentriVap concentrator (Labconco, Kansas City, United States) for 4.5 h at 25 °C. An in-house retention time mixture, with compounds eluting over the entire chromatogram, was injected in between sample measurements and used for the alignment of the bioassay and HRMS results and monitor retention time drifts (Jonkers et al., 2022). A retention time index calibrant was injected at the end of the sequence for retention time modeling with the retention time indices platform, explained in detail

below.

2.3. Antibiotics bioassay

This assay monitors microbial growth inhibition of *E. coli* FhuAT in a 96-well plate format. *E. coli* FhuAT has increased sensitivity to a wide range of antibiotics, as it has an open variant of an outer membrane protein channel and an inactivated multidrug efflux pump (Jonkers et al., 2020). The detailed procedures for the exposures to (un)fractionated extracts have been explained elsewhere (Jonkers et al. 2020, 2022). A summary of the exposure conditions, readout conditions, and calculations of IC50-values is provided in the Supporting Information (Section S3). IC50-values are reported in relative enrichment factors (REFs), referring to the enrichment of the sample corrected for dilution in the bioassay (Escher et al., 2006).

2.4. Calculation of bioanalytical equivalent concentrations

In the bioanalytical equivalent concentrations (BEQ) concept, the bioactivity of a sample is expressed as an equivalent concentration of a reference compound giving the same bioactivity, *i.e.* azithromycin (Table S1). BEQ values can be directly measured in a bioassay (BEQ_{bio}) or be calculated based on the concentration and relative potency (REP) of known bioactive substances in the sample (Neale et al., 2015). For each effluent sample, BEQ_{bio} values were determined by dividing the IC50-value of the reference compound azithromycin (6.4 μg/L) by the IC50-value of the effluent extract of study site A (10.2 REF). BEQ_{chem} values were obtained by multiplying the semi-quantitative concentrations of the identified antimicrobial compounds in the effluent (Table S1) with their respective REP values. For each of the candidate compounds, REP values were determined by dividing the IC50 of the reference compound azithromycin by their respective IC50 in the bioassay.

2.5. Identification of bioactive hits

A fraction was identified as bioactive when its bioassay response differed significantly from that of the procedure blank. As fractions were distributed over the plate in a certain pattern and the plate location of a fraction is the same for every sample, a fraction-dependent bias may have been introduced. To correct for these biases, a generalized additive model (GAM) was fitted to the bioassay chromatogram of the procedure blank. The residuals of the model (corrected for possible variation introduced by the fraction number and plate position) were used to calculate a standard deviation of the procedure blank, which reflected the biological variation of the bioassay and the measurement error (Fig. S2). Fractions in the sample extracts where the bioassay signal deviated significantly from the model (at least ±3x standard deviation) were considered bioactive. A detailed explanation of the algorithm is provided in Section 2 of the Supporting Information. The custom script can be found and downloaded from Github (https://github.com/SystemsBioinformatics/analysis-of-EDA-data).

2.6. Data-processing and feature annotation

2.6.1. Feature extraction

MetaboScape 4.0 (Bruker, Bremen, Germany) was used for the extraction of features and subsequent identification steps. Full scan and MS/MS analyses were processed according to ion mode (positive or negative). Automated mass calibration was performed for each analysis before feature extraction. The software performed a de-isotoping algorithm to generate and extract isotopic patterns (Bruker 2018). Then, it applied a LOESS-based retention time alignment algorithm and arranged the resulting features across the analyses. Recorded MS/MS spectra were automatically assigned to corresponding features. This resulted in two datasets, one for positive and one for negative ion mode measurements. The detailed input settings for MetaboScape are provided in Table S2.

2.6.2. Simulation of phase I antibiotic metabolites

Phase I metabolites were predicted for antibiotics in the 'ITN Antibiotic list' no. S6 of the NORMAN Suspect List Exchange (https://doi.org/10.5281/zenodo.2621957, NORMAN Network 2022). The open-source software BioTransformer (v3.0.0) was used for the metabolite predictions (Djoumbou-Feunang et al., 2019). In the KNIME Analytics Platform (Berthold et al., 2009) QSAR-ready SMILES were prepared, converted to structures, and subsequently to MDL Molfiles, after which they were parsed to CDK format and collated in an SDF file (Mansouri et al., 2016; Meijer et al., 2021). The resulting file, which contained the structures of 505 antibiotic compounds, was imported into the Biotransformer tool, and one-step metabolization predictions were made with the CYP450 function. The predicted metabolites were included as a suspect list in the identification strategy (n = 5710). This suspect list has been published as part of list S6 (ITNANTIBIOTIC) on the NORMAN Suspect List Exchange (https://doi.org/10.5281/zenodo.6511695, Alygizakis and Jonkers 2022; NORMAN Network 2022).

2.6.3. Candidate identification

The annotation workflow was performed according to Jonkers et al. (2022). Features were hierarchically annotated with spectral databases and suspect lists in MetaboScape (Table 1). Features were annotated by matching mass accuracy ($\Delta m/z \leq 10$ ppm), retention time (deviation ≤0.2 min), isotopic pattern fit (mSigma ≤100), and MS/MS score (≥600) to that of a suspect.

The quality of the resulting annotations was assessed using the total annotation quality code (TAQ-code) (Jonkers et al., 2022). The TAQ-code evaluates the mass accuracy, retention time, isotopic pattern fit, and MS/MS spectra similarity of an annotation and additionally includes information on the presence of recorded MS/MS data and whether the feature intensity is ≥ 3x procedure blank (Jonkers et al., 2022). The TAQ-code was also used to assign annotation confidence levels, according to the levels proposed by Schymanski et al. (2014). Level 1 represents a confirmed structure, level 2 represents a probable structure with matching literature or library spectrum data (2a) or diagnostic evidence (2b), level 3 represents tentative candidate(s) (possible structures), level 4 represents an unequivocal molecular formula, and level 5 represents an exact mass (m/z values) (Schymanski et al., 2014). In this paper, level 4 annotations with recorded MS/MS spectra are indicated with an asterisk (4*), as these spectra can be compared to *in silico* predicted molecular fragments.

2.7. Increasing identification confidence with computational tools

2.7.1. MetFrag

MetFrag Web (Ruttkies et al., 2016; Wolf et al., 2010) was used to *in silico* fragment candidate structures. MetFrag predicts structural

Table 1
Suspect lists applied to annotate extracted features.

List	Annotation type	Reference
EU MassBank	SL	NORMAN Network (2022)
MassBank of North America	SL	MoNA (2021)
CECscreen	AL	Meijer et al. (2021), Meijer et al. (2020)
ITNANTIBIOTIC (S6)	AL	Alygizakis (2016), NORMAN Network (2022)
Antibiotic metabolites of S6	AL	This study (Alygizakis and Jonkers 2022; NORMAN Network 2022)
MCS1	AL+	
MCS2	AL+	
Antibiotics1	AL+	

SL = spectral library, AL = analyte suspect list, AL+ = standards, MCS = multicomponent standard.

fragments of an annotated structure and compares that to the recorded fragment spectra of that feature (Ruttkies et al., 2016). A personal candidate database was compiled for a selection of suspect compounds (explained in the Results and Discussion section). The plausibility of predicted bond cleavages for matching predicted and measured fragments was assessed manually.

2.7.2. Retention time predictions

The Retention Time Indices (RTI) platform (Aalizadeh et al., 2021) was used to estimate the retention times of annotations that corresponded to bioactive fractions. The platform applies a quantitative structure–retention relationship (QSRR) model to estimate retention times using the structure of the annotation and the applied chromatographic conditions (Aalizadeh et al., 2021). The Trace Analysis and Mass Spectrometry Group (OTrAMS) (Aalizadeh et al., 2016) and chemical space boundaries (CSB) model (Aalizadeh et al., 2021) were used to estimate the uncertainty of the prediction and the fit within the applicability domain. The OTrAMS model assigns one of four boxes to each estimate, which are related to the standardized residuals (SRs) of the modeling result (Aalizadeh et al., 2016). Structures with matching predicted and measured retention times are assigned to box 1 (up to ±1 SR) or box 2 (between ±1 and ± 2 SRs). Structures with a large prediction error outside the 95% confidence level are assigned to box 3 (between ±2 and ± 3 SRs) or box 4 (between ±3 and ± 4 SRs) (Aalizadeh et al., 2016). The calibration curves, calibrating the retention time index values to the retention times of the individual calibrants of the applied separation method, are presented in Fig. S3.

3. Results and discussion

3.1. Antibiotics assay response to unfractionated and fractionated extracts

All sample extracts of both study sites inhibited bacterial growth in a concentration-dependent manner (Fig. 1). The influent and effluent extracts had complete dose-response curves, with IC50 values of 0.11 and 10 REF for study site A and 0.10 and 7.0 REF for study site B. The surface water extracts had incomplete dose-response curves (the maximum response was not reached at the highest tested REF = 44), thus IC50 values were not calculated. The bioassay responses of the

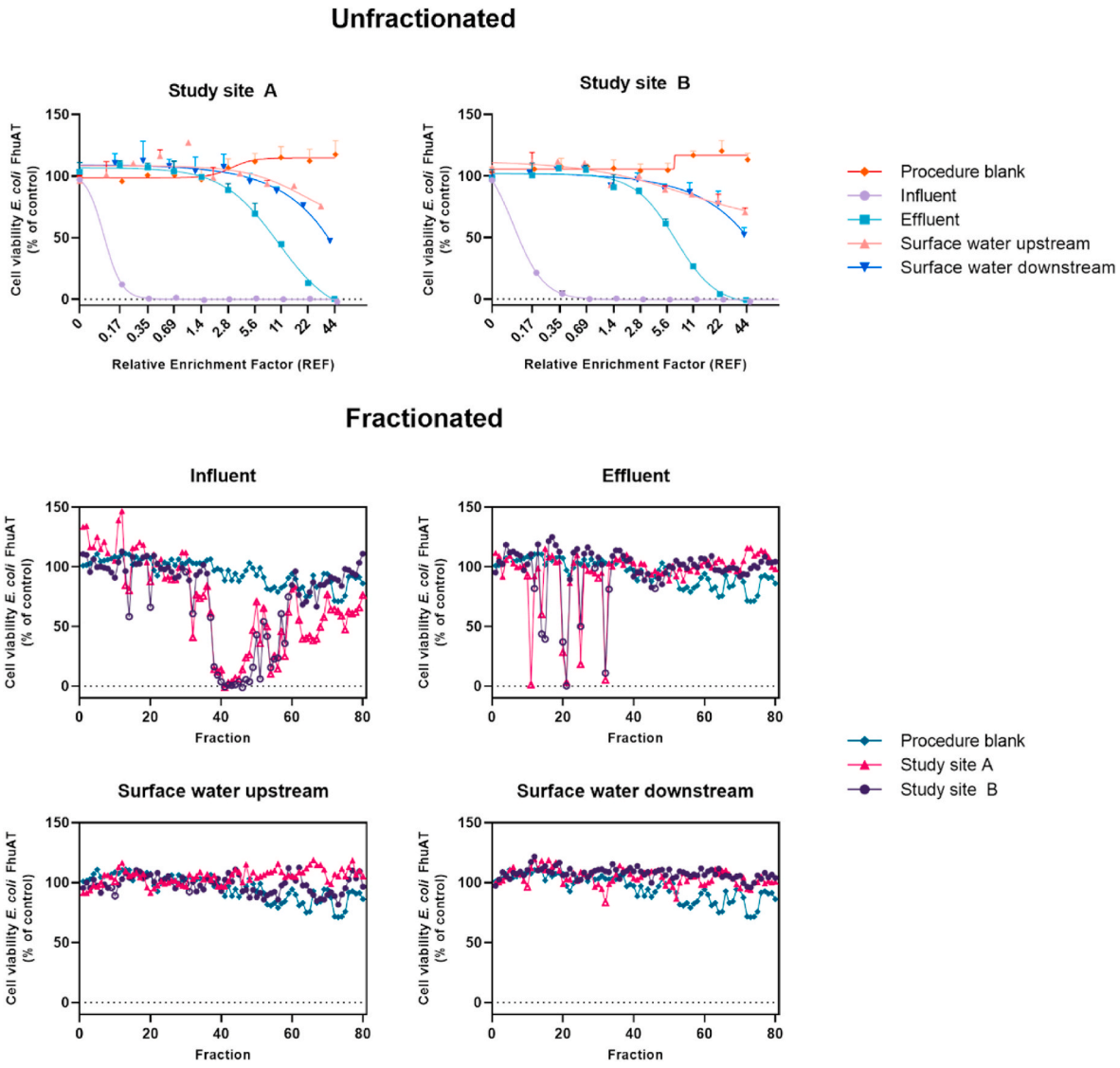

Fig. 1. Antibiotic bioassay responses to the unfractionated and fractionated wastewater influent, wastewater effluent, and surface water collected upstream and downstream of the discharge site for study sites A and B. In the fractionated bioassay results, bioactive fractions are indicated by open markers. Fractions 14, 20, 21, 25, and 32 were bioactive in both fractionated effluent extracts and prioritized. Cell viability values are based on fluorescence measurements, expressing the metabolic activity of *E. coli* FhuAT.

fractionated extracts are presented in Fig. 1. Bioactive fractions in the bioassay chromatograms are presented with open markers (Fig. 1).

Bacterial growth inhibition was observed in the fractionated sample extracts, with most of the bioactivity in the influent and effluent extracts (Fig. 1). Most fractions that were active for the influent extract were inactive for the corresponding effluent extract. The bioactive compounds may have been removed from the influent during wastewater treatment, or transformed into other chemicals with different characteristics. The residence time of wastewater in the WWTPs was not taken into account in the sampling campaign, however, and may partly explain these differences. The effluent extracts demonstrated bioactivity in the more polar fractions that were less active or not active in the influent extracts. This may also have been a result of the different REFs obtained for the two sample types after fractionation, which were 50 for the influent extracts and 300 for the other sample extracts, respectively (Table S3). The compound concentrations may have been too low to inhibit bacterial growth in these fractions. Lower REFs were obtained for the influent extracts as these were reconstituted in a larger volume (compared with the effluent and surface water extracts) to dissolve all of the dried extracts and prevent overloading and clogging of the analytical column. The introduction of more polar transformation products may also partly explain the difference in bioactivity in the influent and effluent bioassay chromatograms. The bioactivity in the polar segment of the effluent extract shows that polar substances may originate from treatment or escape degradation during treatment, or that polar substances are difficult to remove during wastewater treatment (Hale et al., 2020; Reemtsma et al., 2016). Antibiotic standards previously analyzed with this separation method also eluted in the polar segment of the separation method (data not shown). The bioactivity of the fractionated surface water extracts was closer to that of the procedure blank, although some bioactive fractions were identified by the applied algorithm (Fig. 1).

3.2. Annotated features related to bioactive fractions

Bioactive fractions of the effluent extracts were selected for subsequent identification of emerging antimicrobial contaminants. The bioactive fractions in the influent extracts were not selected here, as most of the influent activity was removed during treatment. Five bioactive fractions overlapped between the fractionated effluent extracts of study sites A and B, namely fractions 14, 20, 21, 25, and 32 (Fig. 1). Annotated features were extracted from retention time windows corresponding to these five fractions. Here, a retention time window represented 26.5 s of the MS(MS)-chromatogram per bioactive fraction (the fraction length of 13.5 s with a two-sided error margin of 6.5 s (Jonkers et al., 2022)). Table 2 describes the number of annotations per fraction according to identification confidence level and ion mode.

The annotated features (Table 2) were grouped according to annotation type and prioritized further on measured signal intensities and the deviation between the measured and predicted retention times (Table 3). The annotations were grouped into three categories: parental antibiotics, predicted antibiotic metabolites, and other candidates with possible antimicrobial activity. A signal intensity threshold of 50,000 was applied in the full scan measurements as a prioritization step, considering signal intensity as a proxy for concentration. Further, only annotations with accepted modeled retention time predictions and annotations outside the applicability domain of the RTI model were included in Table 3 (box 1 or 2). Because annotations with identification confidence levels 1 and 2b have matching retention times to the corresponding standards, their retention times were not predicted.

3.2.1. Annotated parental antibiotics

The macrolide antibiotics azithromycin (AZI) and clarithromycin (CLA) were identified at identification confidence level 1 (confirmed structure), by matching to an in-house library of standards. The measured signal intensities of AZI and CLA were among the highest of fractions 21 and 32 of the full scan measurements (ranked as 2nd and 5th for AZI at study sites A and B, ranked 7th and 5th for CLA at study sites A and B, respectively) (data not shown). Both compounds were tested in the antibiotics assay and showed concentration-dependent inhibition of bacterial growth (Fig. S4). The IC50 values were determined to be 8.6 nM (6.4 μg/L) for AZI and 11 nM (8.2 μg/L) for CLA. Standard addition of the effluent extract of study site A was performed with a mixture of analytical standards that included AZI and CLA. This allowed calculating (semi-quantitative) concentrations of AZI and CLA in the extract. The effluent concentrations were estimated by correcting for relative enrichment factors and extraction recoveries; the applied extraction method was validated in earlier experiments (Supporting Information Section S4, Table S6). The effluent concentrations were estimated at 471 ng/L for AZI and 134 ng/L for CLA for study site A. The REF was 315 in the fractionated effluent extract of study site A (Table S3), meaning the exposure concentrations were approximately 105 μg/L for AZI (315 REF x 471 ng/L x 0.71 (71% estimated extraction recovery)) and 33 μg/L for CLA (315 REF x 134 ng/L x 0.78 (78% estimated extraction recovery)). Consequently, AZI and CLA significantly contributed to the bioassay responses of these fractions, as the exposure concentrations exceeded the IC50 concentrations of 6.4 and 8.2 μg/L, respectively.

The lincosamide antibiotic clindamycin was tentatively identified at level 4* by matching it to the 'ITN Antibiotic list' of the NORMAN Suspect List Exchange. The measured signal intensities of this feature were ranked 21st for study site A and 23rd for study site B. The predicted retention time for clindamycin matched with the measured retention time (box 1). Furthermore, three MS/MS fragments were recorded for this feature, which all matched with fragment spectra predicted by MetFrag (Table 3). As such, the identification level of clindamycin was improved from level 4* to level 3. Clindamycin was tested in the antibiotics assay in earlier work and found unable to inhibit bacterial growth up in the *E. coli* FhuAT bioassay up to a test concentration of 40 μg/mL (Jonkers et al., 2020). Clindamycin has a comparable mode of action to chloramphenicol, which is used as a selection marker on a plasmid in *E. coli* FhuAT, possibly affecting the sensitivity to clindamycin (Jonkers et al., 2020). Consequently, the contribution of clindamycin to the bioactivity in the fraction was not investigated further.

Table 2
The number of features related to the selection of bioactive fractions, separated according to identification confidence level. The number of isomers (identified in the CECscreen database) is shown between parentheses.

Identification confidence level	Fraction 14		Fraction 20		Fraction 21		Fraction 25		Fraction 32	
	Pos (n)	Neg (n)	Pos (n)	Neg (n)	Pos (n)	Neg (n)	Pos (n)	Neg (n)	Pos (n)	Neg (n)
Level 1	2	0	0	0	1	0	0	0	2	0
Level 2a	5	0	1	1	2	2	1	0	5	0
Level 2b	1	1	0	0	1	0	1	0	1	0
Level 3	0	0	0	2	0	1	0	3	0	0
Level 4*	4 (27)	13 (25)	15 (46)	19 (31)	10 (55)	19 (27)	9 (178)	25 (178)	3 (15)	21 (74)
Level 4	28 (161)	47 (256)	39 (188)	75 (229)	39 (124)	86 (346)	47 (367)	65 (540)	33 (191)	73 (356)
Level 5	197	387	255	379	274	363	306	274	133	224

Table 3
Annotated features (combined positive and negative ion mode) related to bioactive fractions grouped as parental antibiotics, predicted antibiotic metabolites, and other candidates with possible antimicrobial activity.

Origin	Fraction	Name	Identification confidence level	Number of matching fragments MetFrag[a]	RTI platform
Parental antibiotics	21	Azithromycin	1	n.d.	n.d.
		Clindamycin	4* → 3[d]	3	Box 1
	32	Clarithromycin	1	n.d.	n.d.
Predicted antibiotic metabolites	20	Metampicillin [M1]	4*	1	Box 1
		Bestatin [M1]	4*	2	Box 1
	21	Metampicillin [M1]	4*	1	Box 1
		Azithromycin [M1] (AZI-M1)	4*→ 3[d]	6	Box 2
		Balofloxacin [M1]	4	[b]	[c]
		Sulfapyrazole [M1]	4*	1	Box 1
	25	Clarithromycin [M1-1] (CLA-M1-1)	4* → 3[d]	6	[c]
		Clarithromycin [M3] (CLA-M3)	4* → 3[d]	5	[c]
		Panipenem [M1]	4*	0	Box 2
		Clarithromycin [M1-2] (CLA-M1-2)	4* → 1[d]	5	[c]
	32	Clarithromycin [M2] (CLA-M2)	4* → 3[d]	3	Box 1
		Hydrocortisone 21-acetate [M1]	4	[b]	Box 1
Other candidates	14	1H-benzotriazole	1	n.d.	n.d.
	20	Metolachlor (OA)	4*	4	Box 2
		Benzophenone-4	3 → 1	2	Box 1
	21	Metolachlor oxanilic acid	4*	4	Box 2
	25	Pyrimethanil	2b	[b]	n.d.
	32	DEET	1	n.d.	n.d.

n.d. = not determined: model estimates were not performed for annotations with matching retention times and/or MS/MS fragments to the corresponding analytical standard. M: metabolite. Box 1: accepted experimental and predicted retention times, within ±1 standardized residual of the modeling result. Box 2: accepted experimental and predicted retention times, between ±1 and ± 2 standardized residuals of the modeling result (Aalizadeh et al., 2016).

[a] The number of predicted molecular fragments matching measured fragment masses.

[b] No available measured MS2 data.

[c] Structure was outside the applicability domain of the model, no accurate retention time estimate possible.

[d] The identification confidence level of this annotation was improved by spectra interpretation and/or confirmation.

3.2.2. *Annotated predicted antibiotic metabolites*

In total, fourteen annotated metabolites were prioritized, derivatives of ten unique parent antibiotics (Table 3). The identification confidence levels of five metabolites, all derivatives of AZI or CLA, were increased to level 3 by interpretation of the MS/MS spectra and MetFrag results. The identification confidence level of one metabolite was increased to level 1 and confirmed as bioactive, as explained in detail below. The remaining annotated metabolites had no recorded MS/MS spectra or little matching fragments to the annotated structure and are discussed separately. The applied MS/MS method hierarchically selects precursor ions to fragment based on signal intensity (data-dependent acquisition). As a result, lower intensity signals might not be selected and an additional injection of the sample may be required to collect additional fragmentation data (Jonkers et al., 2022).

3.2.2.1. Annotated clarithromycin metabolites. The predicted metabolic transformation reactions of the annotated CLA metabolites were oxidation (CLA-M1-1 and CLA-M1-2), demethylation (CLA-M2), and oxidation combined with demethylation (CLA-M3). The annotations were related to fraction 25 (CLA-M1-1, CLA-M1-2, CLA-M3) or fraction 32 (CLA, CLA-M2). The MS/MS spectra of CLA and the CLA metabolites were compared to clarify the positions of the predicted (metabolic) changes in the structure of CLA.

For CLA-M1-1 and CLA-M1-2, the observed mass shifts (Δ*m/z*) of the

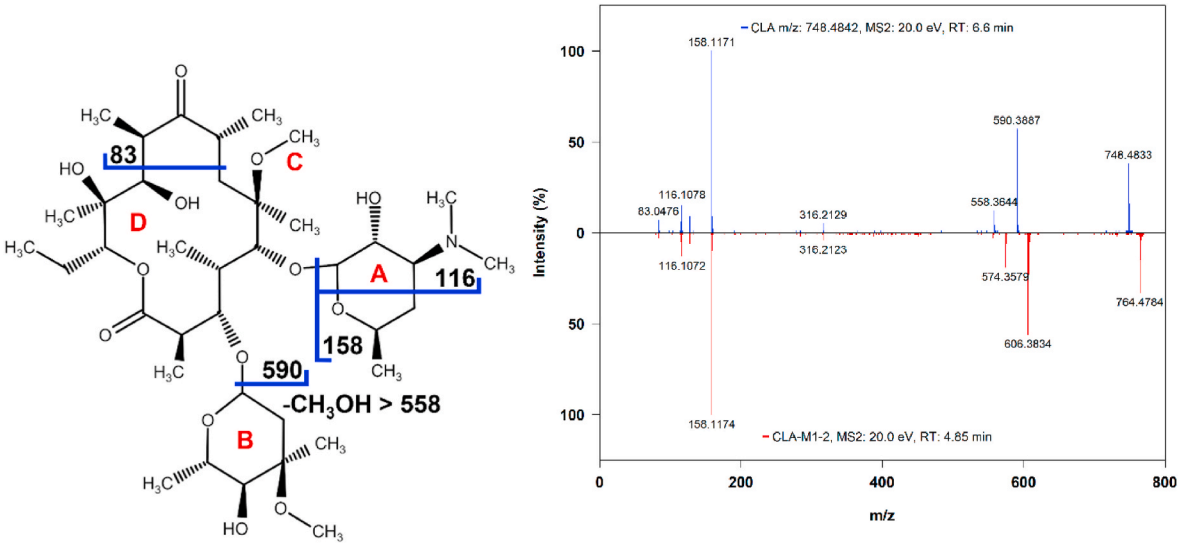

Fig. 2. The structure of CLA (left) and the measured MS/MS spectra of CLA (*m/z* 748.4833, $[M+H]^+$ and metabolite CLA-M1-2 (right, *m/z* 764.4784, $[M+H]^+$), where the relative intensity is plotted against the measured exact masses. A: desosamine moiety (*m/z* 158.1171); B: cladinosyl moiety (158 Da); C: CH_3OH (32 Da); D: macrolide ring.

monoisotopic masses agree with the predicted oxidation reaction ($\Delta m/z$ +16) (Figure S5 and Fig. 2). The mass shifts in the fragments allowed to exclude locations within the structure where oxidation had occurred. For both CLA-M1-1 and CLA-M1-2, the ion with m/z 606 indicates that oxidation was outside the cladinose moiety (corresponding to a loss of 158). The ion with m/z 158 corresponds to the desosamine moiety (Ferrero et al., 1990). As such, the oxidation had occurred in the macrolide ring for both CLA-M1-1 and CLA-M1-2. The ion with m/z 574 (CLA-M1-2) confirms this, as it corresponds to a loss of the cladinose moiety and CH_3OH.

Human metabolism of CLA by the liver involves hydroxylation, resulting in two stereospecific epimers: 14-OH(R) CLA and 14-OH(S) CLA, of which the R form is the most abundant (Davey, 1991; Ferrero et al., 1990). This hydroxylation occurs on the ethyl branch located on the 13th carbon of the macrolide structure (Adachi et al., 1988). The R form has potent antimicrobial activity, whereas the 14-OH(S) metabolite is less active (Adachi et al., 1988).

CLA-M1-2 was confirmed as 14-OH(R) CLA by matching the retention time and MS/MS fragments (including relative intensities) to that of the analytical standard (Table S4). 14-OH (R) CLA was tested in the antibiotics assay and showed comparable potency as CLA (Fig. S4): the IC50 value for 14-OH (R) CLA was determined to be 12 nM (9.1 μg/L). CLA-M1-1 was tentatively identified as 14-OH (S) CLA. The retention times and relative intensities of measured MS/MS fragments differed between CLA-M1-1 and the 14-OH(R) CLA standard (Table S4). The signal intensity of CLA-M1-2 was approximately 3 times higher than that of CLA-M1-1 (data not shown) and corresponded to the abundance of the metabolites after human metabolism (Davey, 1991). As described above, standard addition of the effluent extract was performed and semi-quantitative concentrations of 14-OH(R) CLA were determined. The effluent concentration was estimated at 124 ng/L for 14-OH(R) CLA for study site A. The relative enrichment factor was 315 in the fractionated plate of the effluent extract, meaning the exposure concentration was approximately 28 μg/L for 14-OH(R) CLA (315 REF x 124 ng/L x 0.71 (71% estimated extraction recovery for CLA)). This concentration exceeds the corresponding IC50 value of 9.1 μg/L, meaning 14-OH(R) CLA significantly contributed to the bioassay response of fraction 25.

For CLA-M2, a mass shift of $\Delta m/z$ −14 of the monoisotopic mass was observed compared to CLA (Fig. S6). The $\Delta m/z$ of −14 in the ion with m/z 158 (to m/z 144) indicates N-demethylation. As N-demethylation of CLA inactivates the molecule (Adachi et al., 1988), it was not investigated further.

CLA-M3 showed a mass shift of $\Delta m/z$ +2 in monoisotopic mass (Fig. S7), which is consistent with oxidation and demethylation. The $\Delta m/z$ of −14 in the ion with m/z 158 (to m/z 144) indicates N-demethylation, as with CLA-M2. The loss of −14 also shows that oxidation was outside the (N-demethylated) desosamine moiety. The $\Delta m/z$ of +2 is still present in the ion with m/z 590 (to m/z 592). Thus, the oxidation in CLA-M3 was outside the cladinose ring and must have been in the macrolide ring, as observed for CLA-M1-1 and CLA-M1-2. As oxidation of CLA did not increase the antimicrobial potency and as demethylation of CLA inactivates the molecule, CLA-M3 is not expected to be bioactive and was not investigated further.

3.2.2.2. Annotated azithromycin metabolite. The annotated AZI-M1 metabolite corresponded to the predicted loss of a methyl group, as observed in the $\Delta m/z$ between the monoisotopic of AZI and AZI-M1 from $[M+2H]^{2+}$ m/z 375.2615 to m/z 368.2537 (Fig. S8). Comparing the fragmentation spectra, the $\Delta m/z$ of −14 is observed for the parent ions with m/z 591 and 158. Thus, the $\Delta m/z$ is present after the loss of dehydrocladinose and is observed in the dehydrodesosamine ion with m/z 158. Consequently, N-demethylation has occurred. The ion with m/z 115 is due to the loss of N-methylmethanimine (C_2H_5N) for the parent and due to the loss of methanimine (CH_3N) for the metabolite, confirming N-demethylation. As AZI metabolites are thought to have no bioactivity (Drew and Gallis, 1992), AZI-M1 was not investigated further.

3.2.2.3. Predicted metabolites without annotated parental antibiotics. The identities of the remaining annotated predicted metabolites –for which no parent antibiotics were annotated– were assessed by comparing measured and *in silico* predicted molecular fragments using MetFrag. The detailed prediction results are included in the Supporting Information. Panipenem M1 lacked matching MS/MS fragments between the measured and predicted data. Metampicillin M1 and sulfapyrazole M1 had matching fragments, but the predicted cleavages by MetFrag were unlikely to occur (*i.e.* the loss of hydroxyl as the most abundant fragment ion and the loss of double-bound oxygen, respectively). Some annotations lacked recorded MS/MS spectra (level 4 annotations) as the precursor ions were not selected for fragmentation by the applied DDA method. Therefore, the effluent extract of location A was re-analyzed. For balofloxacin M1 and hydrocortisone 21-acetate M1 no fragmentation data could be obtained, although fragmentation data were collected for the feature annotated as bestatin M1. Two predicted fragments matched with the recorded fragments, but represented cleavages within the benzene ring of bestatin M1, and were as such unlikely to occur. These features were probably incorrectly annotated as antibiotic metabolites considering the absence of likely molecular fragments between the measured and predicted fragments, and supported by the absence of annotated parental molecules.

3.2.3. Other annotations with possible antimicrobial activity

The bioactivity of fractions 14 and 20 cannot be explained by the annotations of (predicted metabolites of) antibiotics. For these fractions, candidates with possible antimicrobial activity were selected based on their reported uses. The annotations 1H-benzotriazole (identification confidence level 1, by matching to an in-house library of standards), metolachlor oxanilic acid (level 4*), and benzophenone-4 (level 3) were selected as candidates accordingly. For certain benzotriazole and benzophenone derivatives antimicrobial activity has been reported (Briguglio et al., 2015; Hong and Sun, 2008), and metolachlor oxanilic acid is a metabolite of the herbicide metolachlor (Phillips et al., 1999). Analytical standards of these selected candidates were used for chemical analysis and bioactivity testing in the antibiotics assay. The chemical identity of benzophenone-4 was confirmed based on matching retention times and fragmentation patterns. The retention time for metolachlor oxanilic acid differed more than 2 min with its spiked standard, however, and had different MS/MS fragments. Regarding bioactivity, compounds 1-H benzotriazole and benzophenone-4 showed no significant antimicrobial activity in the *E. coli* FhuAT antibiotics assay up to a test concentration of 100 mg/L (data not shown). These effluent concentrations (study site A) were semi-quantified at 519 ng/L for 1H-benzotriazole and 393 ng/L for benzophenone-4 by applying standard addition (uncorrected for extraction recoveries). Then, exposure concentrations in the fractionated plates were approximately 163 μg/L for 1-H benzotriazole and 124 μg/L for benzophenone-4 (315 REF x concentration). As such, it is unlikely that 1H-benzotriazole and benzophenone-4 contributed to the bioactivity of either fraction 14 or 20. The corrosion inhibitor 1-H benzotriazole is among the most frequently detected polar compounds within European effluents, often in the μg/L range (Loos et al., 2013). The UV-filter benzophenone-4 has also frequently been detected in effluents in this concentration range (Ramos et al., 2016).

The applied workflow was unable to confirm bioactive components in fractions 14 and 20, which may have several reasons. It could be that chemical features remained unannotated and were consequently not prioritized. Or, that annotated features were not prioritized for confirmation based on their (manually assessed) use. The majority of features associated with each fraction had identification confidence levels of 5 (Table 2). Unannotated features were not prioritized and considered,

which is a limitation of the applied study design. In future studies, two strategies may be applied to overcome this issue. First, *in silico*-generated phase-II metabolites could be included in the suspect screening lists. Fractions 14 and 20 were the most polar of the studied fractions and may be related to the activity of more polar metabolites. In parallel, the chemical composition of level 5 features with high signal intensities, as a proxy for concentration, could be estimated. The estimated elemental composition can be used to assign a chemical identity by matching with larger compound databases such as PubChemLite (Schymanski et al., 2021) or ChemSpider (RSC, 2022), and match measured fragmentation data to *in silico* predicted MS/MS spectra. Also, the high number of annotations per fraction (Table 1) shows that, rather than manually searching candidates on reported uses, a structure-based prioritization step on effect could further improve candidate selection for confirmation. For example, a model that can estimate the antimicrobial potency of an annotated structure based on compound class annotations (Dührkop et al., 2021). Or, by integrating bioactivity models as included in ToxCast for toxicological endpoints such as estrogen and androgen activity (USEPA, 2022).

3.2.4. Bioactive compounds in influent and surface water samples

CLA and AZI were detected in the influent samples although 14-OH (R) CLA was not (Table S5), whereas CLA and 14-OH(R) CLA are both mainly excreted via urine in similar amounts (Ferrero et al., 1990). This may be explained by the lower relative enrichment factor of the influent samples and by matrix effects leading to ion suppression in the MS measurements. The formation of the 14-OH(R) metabolite during wastewater treatment cannot be excluded but is unlikely, as the ratio between signal intensities corresponded to the abundance of metabolites after human metabolism (Davey, 1991), as discussed above.

CLA and 14-OH(R) CLA were detected in the surface water samples, both up and downstream of the discharge location. AZI was only identified in the surface water extracts of study site A. The signal intensities of these bioactive compounds (shown in Table S5) were a factor 2–6 higher in extracts from downstream than from upstream water extracts of study site A (Table S5), whereas there was no difference for study site B. This difference could be due to sampling, however, as the surface water samples were grab samples. Of the five studied bioactive fractions, only fraction 32 was bioactive in the downstream effluent extract of study site A, in which CLA was identified. As AZI (study site A) and 14-OH(R) CLA (study site A and B) were chemically identified in the surface water samples, the REFs of the fractionated surface water samples were too low for AZI and 14-OH(R) CLA to significantly inhibit bacterial growth.

The antibiotics that were detected in the upstream surface water samples may have been introduced by varying point sources, including a WWTP located ~28 km upstream of study site A that also discharges on this surface water. The effluent of study site A may also have diluted both up and downstream of the discharge location if the river flow was low.

3.3. Contribution of the identified chemicals to the unfractionated bioassay response

The contribution of AZI, CLA, and 14-OH(R) CLA to the unfractionated bioassay response of the effluent extract (study site A) was estimated using the bioanalytical equivalent concentration (BEQ) concept. Although BEQ_{chem} is based on semi-quantitative concentrations, the effluent concentrations of AZI (471 ng/L), CLA (134 ng/L), and 14-OH CLA (124 ng/L) were comparable with previously reported concentrations in European effluents (*i.e.* within the range of 3–1060 ng/L) (Alygizakis et al., 2019; Senta et al., 2017; Wang et al., 2020) and as such accepted for calculating BEQ_{chem} values. Overall, AZI, CLA, and 14-OH(R) CLA contributed to 78% of the effect observed in the bioassay of the unfractionated effluent extract of study site A.

3.4. European environmental monitoring of CLA, AZI, and 14-OH(R) CLA

Macrolide antibiotics have been detected in the aquatic environment worldwide (Li et al., 2020). In 2015, the macrolide antibiotics AZI and CLA were included on the EU Watchlist under the Water Framework Directive, because high-quality monitoring data were lacking on their occurrence in European surface waters (Eur, 2020; Loos et al., 2018). Currently, the (restricted) monitoring period of four years has concluded. From the collected data, the median surface water concentrations in Europe were determined to be 0.022 μg/L for AZI and 0.016 μg/L for CLA. The corresponding Predicted No Effect Concentration (PNEC) values are 0.019 μg/L for AZI and 0.12 μg/L for CLA (Loos et al., 2018). Because AZI currently poses an environmental risk at EU level, there is a need for (risk) management measures on how to deal with this substance in the environment.

The EU technical guideline for deriving environmental quality standards does not consider transformation products (EC, 2018). Nonetheless, in the PNEC derivation of CLA (or annual average quality standard), an additional assessment factor of 2 has been applied to address the toxicity of transformation products including the metabolite 14-OH CLA (SCHEER, 2022; UBA, 2014). The scientific committee on health, environmental and emerging risks (SCHEER) has recently requested a more detailed motivation for the selection of this factor 2 in the derivation of the acute maximum acceptable concentration quality standard (SCHEER, 2022). In the current study, the BEQ_{chem} of 14-OH (R) CLA (0.068 μg/L) represented 83% of its parent CLA (0.082 μg/L). The suggested additional assessment factor of 2 would, in this study, therefore be adequate to cover the bioactivity of the 14-OH(R) CLA metabolite in the PNEC derivation of CLA.

4. Conclusions

An antibiotics assay identified antimicrobial activity in fractionated (waste)water samples. Using open (software) tools including BioTransformer, the retention time indices platform, MetFrag, and the NORMAN Network Suspect List Exchange, chemical features were tentatively identified and prioritized to increase identification confidence levels of the compounds causing the activity. A suspect list of predicted antibiotic metabolites developed for this study supported the identification of the bioactive human metabolite 14-OH(R) CLA. This finding showed that the applied EDA workflow is suitable to detect and identify biologically active pharmaceutical metabolites. The bioactivity of 3 out of 5 fractions –that were prioritized– was explained by identified antibiotic compounds or derivatives thereof. Approximately 78% of the bioassay activity (of one sample and study site) could be explained by the identified compounds of that sample. The occurrence of bioactive metabolites in surface water emphasizes the need to include the toxic effects of bioactive metabolites in the environmental risk assessments of the parent compound. Substances prioritized with the workflow but found to be inactive (such as 1H-benzotriazole and benzophenone) highlight the need for confirmation of compounds in EDA studies with analytical standards, biologically and chemically. Modeled approaches to the studied toxicological endpoint(s) and annotated structures, may further improve the throughput and prioritization of (novel) bioactive compounds in future EDA studies.

Author statement

Tim J.H. Jonkers: Conceptualization, Methodology, Software, Formal Analysis, Investigation, Writing - original draft. Peter H.J. Keizers: Conceptualization, Investigation, Writing - review & editing. Frederic Béen: Resources, Writing - review & editing. Jeroen Meijer: Conceptualization, Writing - review & editing. Corine J. Houtman: Writing - review & editing, Supervision, Funding acquisition. Imane Al Gharib: Methodology, Software, Investigation. Douwe Molenaar:

Conceptualization, Data Curation. Timo Hamers: Conceptualization, Methodology, Writing - review & editing, Supervision. Marja H. Lamoree: Conceptualization, Methodology, Writing - review & editing, Supervision, Funding acquisition.

Declaration of competing interest

The authors declare that they have no known competing financial interests or personal relationships that could have appeared to influence the work reported in this paper.

Data availability

Data will be made available on request.

Acknowledgements

The authors gratefully acknowledge Dr. Wilfried Niessen (hyphen MassSpec) for the assistance in the interpretation of the fragmentation spectra. This work is part of the research program RoutinEDA with project number 15747, which is (partly) financed by the Dutch Research Council (NWO).

Appendix A. Supplementary data

Supplementary data to this article can be found online at https://doi.org/10.1016/j.chemosphere.2023.138093.

References

Aalizadeh, R., Thomaidis, N.S., Bletsou, A.A., Gago-Ferrero, P., 2016. Quantitative structure–retention relationship models to support nontarget high-resolution mass spectrometric screening of emerging contaminants in environmental samples. J. Chem. Inf. Model. 56 (7), 1384–1398.

Aalizadeh, R., Alygizakis, N.A., Schymanski, E.L., Krauss, M., Schulze, T., Ibáñez, M., McEachran, A.D., Chao, A., Williams, A.J., Gago-Ferrero, P., Covaci, A., Moschet, C., Young, T.M., Hollender, J., Slobodnik, J., Thomaidis, N.S., 2021. Development and application of liquid chromatographic retention time indices in HRMS-based suspect and nontarget screening. Anal. Chem. 93 (33), 11601–11611.

Adachi, T., Morimoto, S., Kondoh, H., Nagate, T., Watanabe, Y., Sota, K., 1988. 14-Hydroxy-6-O-methylerythromycins A, active metabolites of 6-O-methylerythromycin A in human. J. Antibiot. 41 (7), 966–975.

Alygizakis, N., 2016. S6 | ITNANTIBIOTIC | Antibiotic List: ITN MSCA ANSWER (NORMAN-SLE-S6.0.1.0). https://doi.org/10.5281/zenodo.2621957. Zenodo.

Alygizakis, N.A., Besselink, H., Paulus, G.K., Oswald, P., Hornstra, L.M., Oswaldova, M., Medema, G., Thomaidis, N.S., Behnisch, P.A., Slobodnik, J., 2019. Characterization of wastewater effluents in the Danube River Basin with chemical screening, in vitro bioassays and antibiotic resistant genes analysis. Environ. Int. 127, 420–429.

Alygizakis, Jonkers, N.T., 2022. S6 | ITNANTIBIOTIC | Antibiotic List: ITN MSCA ANSWER (NORMAN-SLE-S6.0.2.0) Zenodo. https://doi.org/10.5281/zenodo.6511695.

Bruker, 2018. MetaboScape 4.0 User Manual. Bruker Daltonik GmbH.

EC, 2018. Technical Guidance for Deriving Environmental Quality Standards. European Commission, pp. 1–208.

EC, 2019. European Union Strategic Approach to Pharmaceuticals in the Environment. European Commission, Brussels.

Bengtsson-Palme, J., Larsson, D.G.J., 2016. Concentrations of antibiotics predicted to select for resistant bacteria: proposed limits for environmental regulation. Environ. Int. 86, 140–149.

Berthold, M.R., Cebron, N., Dill, F., Gabriel, T.R., Kötter, T., Meinl, T., Ohl, P., Thiel, K., Wiswedel, B., 2009. KNIME - the Konstanz information miner: version 2.0 and beyond. SIGKDD Explor. Newsl. 11 (1), 26–31.

Briguglio, I., Piras, S., Corona, P., Gavini, E., Nieddu, M., Boatto, G., Carta, A., 2015. Benzotriazole: an overview on its versatile biological behavior. Eur. J. Med. Chem. 97, 612–648.

Davey, P.G., 1991. The pharmacokinetics of clarithromycin and its 14-OH metabolite. J. Hosp. Infect. 19, 29–37.

Djoumbou-Feunang, Y., Fiamoncini, J., Gil-de-la-Fuente, A., Greiner, R., Manach, C., Wishart, D.S., 2019. BioTransformer: a comprehensive computational tool for small molecule metabolism prediction and metabolite identification. J. Cheminf. 11 (1), 2.

Drew, R.H., Gallis, H.A., 1992. Azithromycin—spectrum of activity, pharmacokinetics, and clinical applications. Pharmacotherapy 12 (3), 161–173.

Dührkop, K., Nothias, L.-F., Fleischauer, M., Reher, R., Ludwig, M., Hoffmann, M.A., Petras, D., Gerwick, W.H., Rousu, J., Dorrestein, P.C., Böcker, S., 2021. Systematic classification of unknown metabolites using high-resolution fragmentation mass spectra. Nat. Biotechnol. 39 (4), 462–471.

Escher, B.I., Fenner, K., 2011. Recent advances in environmental risk assessment of transformation products. Environ. Sci. Technol. 45 (9), 3835–3847.

Escher, B.I., Quayle, P., Muller, R., Schreiber, U., Mueller, J.F., 2006. Passive sampling of herbicides combined with effect analysis in algae using a novel high-throughput phytotoxicity assay (Maxi-Imaging-PAM). J. Environ. Monit. 8 (4), 456–464.

Escher, B.I., Stapleton, H.M., Schymanski, E.L., 2020. Tracking complex mixtures of chemicals in our changing environment. Science (New York, N.Y.) 367 (6476), 388–392.

Eur, E., 2020. Commission Implementing Decision (EU) 2020/1161 of 4 August 2020 Establishing a Watch List of Substances for Union-wide Monitoring in the Field of Water Policy Pursuant to Directive 2008/105. EC of the European Parliament and of the Council, pp. 32–35.

Ferrero, J.L., Bopp, B.A., Marsh, K.C., Quigley, S.C., Johnson, M.J., Anderson, D.J., Lamm, J.E., Tolman, K.G., Sanders, S.W., Cavanaugh, J.H., 1990. Metabolism and disposition of clarithromycin in man. Drug Metabol. Dispos. 18 (4), 441–446.

Fu, L., Huang, T., Wang, S., Wang, X., Su, L., Li, C., Zhao, Y., 2017. Toxicity of 13 different antibiotics towards freshwater green algae Pseudokirchneriella subcapitata and their modes of action. Chemosphere 168, 217–222.

Gros, M., Rodríguez-Mozaz, S., Barceló, D., 2013. Rapid analysis of multiclass antibiotic residues and some of their metabolites in hospital, urban wastewater and river water by ultra-high-performance liquid chromatography coupled to quadrupole-linear ion trap tandem mass spectrometry. J. Chromatogr. A 1292, 173–188.

Hale, S.E., Arp, H.P.H., Schliebner, I., Neumann, M., 2020. What's in a name: persistent, mobile, and toxic (PMT) and very persistent and very mobile (vPvM) substances. Environ. Sci. Technol. 54 (23), 14790–14792.

Hamers, T., Kamstra, J.H., van Gils, J., Kotte, M.C., van Hattum, A.G.M., 2015. The influence of extreme river discharge conditions on the quality of suspended particulate matter in Rivers Meuse and Rhine (The Netherlands). Environ. Res. 143, 241–255.

Hong, K.H., Sun, G., 2008. Antimicrobial and chemical detoxifying functions of cotton fabrics containing different benzophenone derivatives. Carbohydr. Polym. 71 (4), 598–605.

Houtman, C.J., ten Broek, R., Brouwer, A., 2018. Steroid hormonal bioactivities, culprit natural and synthetic hormones and other emerging contaminants in waste water measured using bioassays and UPLC-tQ-MS. Sci. Total Environ. 630, 1492–1501.

Jonker, W., de Vries, K., Althuisius, N., van Iperen, D., Janssen, E., ten Broek, R., Houtman, C., Zwart, N., Hamers, T., Lamoree, M.H., Ooms, B., Hidding, J., Somsen, G.W., Kool, J., 2019. Compound identification using liquid chromatography and high-resolution noncontact fraction collection with a solenoid valve. SLAS Technol. 24 (6), 543–555.

Jonkers, T.J.H., Steenhuis, M., Schalkwijk, L., Luirink, J., Bald, D., Houtman, C.J., Kool, J., Lamoree, M.H., Hamers, T., 2020. Development of a high-throughput bioassay for screening of antibiotics in aquatic environmental samples. Sci. Total Environ. 729, 139028.

Jonkers, T.J.H., Meijer, J., Vlaanderen, J.J., Vermeulen, R.C.H., Houtman, C.J., Hamers, T., Lamoree, M.H., 2022. High-Performance data processing workflow incorporating effect-directed analysis for feature prioritization in suspect and nontarget screening. Environ. Sci. Technol. 56 (3), 1639–1651.

Li, J., Li, W., Liu, K., Guo, Y., Ding, C., Han, J., Li, P., 2020. Global review of macrolide antibiotics in the aquatic environment: sources, occurrence, fate, ecotoxicity, and risk assessment. J. Hazard Mater. 439 (2022), 129628.

Loos, R., Carvalho, R., António, D.C., Comero, S., Locoro, G., Tavazzi, S., Paracchini, B., Ghiani, M., Lettieri, T., Blaha, L., Jarosova, B., Voorspoels, S., Servaes, K., Haglund, P., Fick, J., Lindberg, R.H., Schwesig, D., Gawlik, B.M., 2013. EU-wide monitoring survey on emerging polar organic contaminants in wastewater treatment plant effluents. Water Res. 47 (17), 6475–6487.

Loos, R., Marinov, D., Sanseverino, I., Napierska, D., Lettieri, T., 2018. Review of the 1st Watch List under the Water Framework Directive and Recommendations for the 2nd Watch List. Publications Office of the European Union, Luxembourgh, p. 265.

Mansouri, K., Grulke, C.M., Richard, A.M., Judson, R.S., Williams, A.J., 2016. An automated curation procedure for addressing chemical errors and inconsistencies in public datasets used in QSAR modelling. SAR QSAR Environ. Res. 27 (11), 911–937.

Meijer, J.L., Lamoree, Marja, Hamers, Timo, Antingac, Jean-Philippe, Hutinet, Sébastien, Debrauwer, Laurent, Covaci, Adrian, Huber, Carolin, Krauss, Martin, Walker, Douglas I., Schymanski, Emma, Vermeulen, Roel, Vlaanderen, Jelle, 2020. S71 | CECSCREEN | HBM4EU CECscreen: screening list for chemicals of emerging concern plus metadata and predicted phase 1 metabolites. Zenodo. https://doi.org/10.5281/zenodo.3957497.

Meijer, J., Lamoree, M., Hamers, T., Antignac, J.-P., Hutinet, S., Debrauwer, L., Covaci, A., Huber, C., Krauss, M., Walker, D.I., Schymanski, E.L., Vermeulen, R., Vlaanderen, J., 2021. An annotation database for chemicals of emerging concern in exposome research. Environ. Int. 152, 106511.

MoNA, 2021. Massbank of North America. Massbank of North America. https://mona.fiehnlab.ucdavis.edu/.

Neale, P.A., Ait-Aissa, S., Brack, W., Creusot, N., Denison, M.S., Deutschmann, B., Hilscherová, K., Hollert, H., Krauss, M., Novák, J., Schulze, T., Seiler, T.-B., Serra, H., Shao, Y., Escher, B.I., 2015. Linking in vitro effects and detected organic micropollutants in surface water using mixture-toxicity modeling. Environ. Sci. Technol. 49 (24), 14614–14624.

Neale, P.A., Munz, N.A., Aït-Aïssa, S., Altenburger, R., Brion, F., Busch, W., Escher, B.I., Hilscherová, K., Kienle, C., Novák, J., Seiler, T.-B., Shao, Y., Stamm, C., Hollender, J., 2017. Integrating chemical analysis and bioanalysis to evaluate the contribution of wastewater effluent on the micropollutant burden in small streams. Sci. Total Environ. 576, 785–795.

NORMAN Network, 2022. NORMAN Suspect List Exchange (NORMAN-SLE). https://www.norman-network.com/nds/SLE/.

Petrie, B., Barden, R., Kasprzyk-Hordern, B., 2015. A review on emerging contaminants in wastewaters and the environment: current knowledge, understudied areas and recommendations for future monitoring. Water Res. 72, 3–27.
Phillips, P.J., Wall, G.R., Thurman, E.M., Eckhardt, D.A., 1999. Metolachlor and its metabolites in tile drain and stream runoff in the canajoharie creek watershed. Environ. Sci. Technol. 33 (20), 3531–3537.
Ramos, S., Homem, V., Alves, A., Santos, L., 2016. A review of organic UV-filters in wastewater treatment plants. Environ. Int. 86, 24–44.
Reemtsma, T., Berger, U., Arp, H.P.H., Gallard, H., Knepper, T.P., Neumann, M., Quintana, J.B., Voogt, P.d., 2016. Mind the gap: persistent and mobile organic compounds—water contaminants that slip through. Environ. Sci. Technol. 50 (19), 10308–10315.
RSC, 2022. ChemSpider Search and Share Chemistry. Royal Society of Chemistry.
Ruttkies, C., Schymanski, E.L., Wolf, S., Hollender, J., Neumann, S., 2016. MetFrag relaunched: incorporating strategies beyond in silico fragmentation. J. Cheminf. 8 (1), 3.
SCHEER, 2022. Draft Environmental Quality Standards for Priority Substances under the Water Framework Directive" - Clarithromycin.
Schymanski, E.L., Jeon, J., Gulde, R., Fenner, K., Ruff, M., Singer, H.P., Hollender, J., 2014. Identifying small molecules via high resolution mass spectrometry: communicating confidence. Environ. Sci. Technol. 48 (4), 2097–2098.
Schymanski, E.L., Kondić, T., Neumann, S., Thiessen, P.A., Zhang, J., Bolton, E.E., 2021. Empowering large chemical knowledge bases for exposomics: PubChemLite meets MetFrag. J. Cheminf. 13 (1), 19.
Senta, I., Krizman-Matasic, I., Terzic, S., Ahel, M., 2017. Comprehensive determination of macrolide antibiotics, their synthesis intermediates and transformation products in wastewater effluents and ambient waters by liquid chromatography–tandem mass spectrometry. J. Chromatogr. A 1509, 60–68.
Serra-Compte, A., Pikkemaat, M.G., Elferink, A., Almeida, D., Diogène, J., Campillo, J.A., Llorca, M., Álvarez-Muñoz, D., Barceló, D., Rodríguez-Mozaz, S., 2021. Combining an effect-based methodology with chemical analysis for antibiotics determination in wastewater and receiving freshwater and marine environment. Environ. Pollut. 271, 116313.
UBA, 2014. EQS Datasheet Environmental Quality Standard Clarithromycin (Umweltbundesamt).
USEPA, 2022. Toxcast & Tox21. U.S. Environmental Protection Agency.
Wang, J., Chu, L., Wojnárovits, L., Takács, E., 2020. Occurrence and fate of antibiotics, antibiotic resistant genes (ARGs) and antibiotic resistant bacteria (ARB) in municipal wastewater treatment plant: an overview. Sci. Total Environ. 744, 140997.
Wengenroth, L., Berglund, F., Blaak, H., Chifiriuc, M.C., Flach, C.-F., Pircalabioru, G.G., Larsson, D.G.J., Marutescu, L., van Passel, M.W.J., Popa, M., Radon, K., de Roda Husman, A.M., Rodríguez-Molina, D., Weinmann, T., Wieser, A., Schmitt, H., 2021. Antibiotic resistance in wastewater treatment plants and transmission risks for employees and residents: the concept of the AWARE study. Antibiotics 10 (5), 478.
Wolf, S., Schmidt, S., Müller-Hannemann, M., Neumann, S., 2010. In silico fragmentation for computer assisted identification of metabolite mass spectra. BMC Bioinf. 11 (1), 148.
Zwart, N., Nio, S.L., Houtman, C.J., de Boer, J., Kool, J., Hamers, T., Lamoree, M.H., 2018. High-throughput effect-directed analysis using downscaled in vitro reporter gene assays to identify endocrine disruptors in surface water. Environ. Sci. Technol. 52 (7), 4367–4377.